

Variation of thin film edge magnetic properties with patterning process conditions in $\text{Ni}_{80}\text{Fe}_{20}$ stripes

Brian B. Maranville^{a)} and Robert D. McMichael^{b)}

Metallurgy Division, National Institute of Standards and Technology, 100 Bureau Drive, Gaithersburg, Maryland 20899

David W. Abraham

IBM Thomas J. Watson Research Center, P.O. Box 218, Yorktown Heights, New York 10598

(Received 27 March 2007; accepted 11 May 2007; published online 6 June 2007)

The authors report the effect of etch depth on the magnetic properties of thin film edges in magnetic nanostructures. In transversely magnetized stripes of 20-nm-thick $\text{Ni}_{80}\text{Fe}_{20}$, they use ferromagnetic resonance spectroscopy to measure the edge saturation field and effective out-of-plane stiffness field of the trapped-spin-wave edge mode as a function of ion etch depth. With increasing etching depth, the edge surface angle changes from 47° to 80° , and the field required to saturate the edge magnetization perpendicular to the stripe axis nearly doubles. This trend is largely confirmed by micromagnetic modeling of the edge geometry. © 2007 American Institute of Physics.

[DOI: 10.1063/1.2746406]

The discovery of giant magnetoresistance, the rapid developments in tunneling magnetoresistance, and the emergence of spin-transfer torque as a rapidly growing field of study have spurred great interest in patterning and characterization of magnetic thin film devices. In many magnetic thin film devices, the magnetic properties of the film edge play a critical role in the magnetic behavior of the device, and the patterning conditions¹ or postpatterning treatments of the film edges² have been shown to affect the switching properties in device arrays.

The edges influence the switching behavior in different ways for different device sizes. In devices that are many times larger than an exchange length $l_{\text{ex}} = (2A/\mu_0 M_s^2)^{1/2}$, magnetization reversal often occurs via nucleation of a vortex at the film edge, where the edge properties are dominant.^{1,3-7} The edge properties are also important in smaller structures, where reversal takes place by other mechanisms⁸⁻¹⁰ including nearly uniform rotation.² The edges in these small structures are important by virtue of the fact that more of the device material is near a film edge.

Despite the important role of edges in magnetic nanostructures, there have been only a few direct measurements of the magnetic properties of thin film edges.^{11,12} The edge property measurements we report here are based on the developments in the magnetization dynamics in nanostructures. These studies have revealed the existence of localized precession modes in the low-field region near a film edge, when the applied field is oriented in plane and perpendicular to the edge.¹²⁻¹⁷ Previous modeling of the edge modes has shown that the localized “edge mode” is sensitive to the edge properties, and among other effects, that the edge mode is sensitive to the sidewall angle θ_e that measures the tilting of the edge surface from vertical.^{15,18} In this letter we present a report of the effects of processing conditions on the quantitative magnetic properties of thin film edges.

A 20 nm thick film of $\text{Ni}_{80}\text{Fe}_{20}$ capped with 5 nm of Ru was sputter deposited onto thermal silicon oxide on a Si

substrate. The film was patterned into an array of 240-nm-wide stripes with period of 680 nm by Ar ion milling through a photoresist mask. During the etch, the samples were placed in the center of a rotating stage oriented 45° to the ion beam. Redeposited material, evident in micrographs, could be largely removed using light swabbing in an isopropyl alcohol without affecting the magnetic measurements. The etch depth and sidewall angle θ_e were measured by atomic force microscopy using a tip that is canted 35° from vertical. Resolution is limited by 10 nm nominal radius of the tip. The etch depth increased linearly with etch time, and the sidewall angle increased from approximately 47° , when the exposed film was just etched through, to approximately 80° when the etch depth was 3.5 times the film thickness, as shown in Fig. 1.

The magnetic properties of the sample edges are determined by the microwave-frequency ferromagnetic resonance (FMR) of the stripe array in the presence of a large quasi-static field H_0 applied perpendicular to the stripes (see the inset in Fig. 2). The samples are held in place on a coplanar waveguide using a thin layer of vacuum grease which prevents shorting of the waveguide. Detection of the FMR modes is achieved by measuring the changes in the transmission of the waveguide. When the combination of applied field H_0 and excitation frequency f corresponds to a resonance, the microwave field h_{rf} drives precession of the magnetization, energy is dissipated by magnetic damping processes, and the transmission of the waveguide is correspondingly reduced. Signal to noise is improved by adding a small oscillating modulation field $h_{\text{mod}}(t)$ with frequency 77 Hz and approximate amplitude of 1 mT, and by using a lock-in amplifier to analyze the modulated part of the transmitted signal.

A typical field-swept spectrum is shown at the top part of Fig. 2. Comparison with the micromagnetic modeling of the modes and their profiles allows us to identify the more intense resonance as one or more overlapping bulk modes and the weaker resonance as the edge mode.

Straight edges and accurate alignment are needed to measure the edge mode resonance at low frequencies.¹² To

^{a)}Electronic mail: bbm@nist.gov

^{b)}Electronic mail: rmc michael@nist.gov

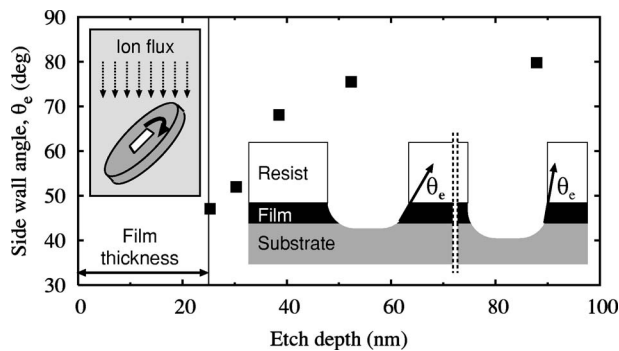


FIG. 1. Atomic force microscopy profiles show that sidewall angle increases with etch depth. A possible mechanism is sketched in the right inset. The etching configuration is shown on the left.

assess the straightness of the stripes, we used the angular dependence of the remanent magnetization.¹¹ We found that the remanent magnetization changed from one direction along the stripes to the other within less than 1° of applied field angle for all samples. Field alignment was facilitated by mounting the waveguide and sample on a stepper-motor-driven platform with a precision of 0.1° . The optimum orientation is determined by maximizing the edge mode resonance field as a function of applied field angle, with a precision of approximately 0.2° .

Multiple FMR spectra are used to build mode maps such as the one shown in Fig. 2. The equilibrium magnetization lies parallel to the stripes in zero field and rotates toward the perpendicular in-plane direction as H_0 is increased. The minimum in the resonance frequency at 0.09 T corresponds to the saturation of the magnetization in the center of the stripes parallel to H_0 . The deeper minimum in Fig. 2 occurs at the field H_{sat} where the edge magnetization is saturated perpendicular to the edges.^{15,19} At this field, the edge magnetization is just barely stable, with the stabilizing effects of the applied field and exchange coupling to the bulk just balancing the destabilizing effect of the demagnetization field near the edge.

For fields above H_{sat} , the lower frequency resonance is the edge mode, and the higher frequency mode is due to one

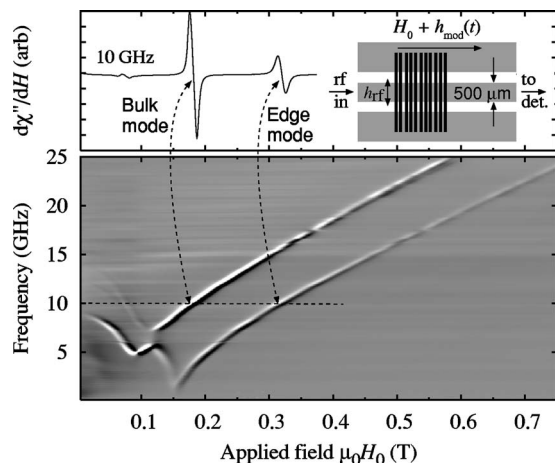


FIG. 2. Top: FMR spectrum of the stripe array with 39 nm etch depth measured at 10 GHz. The high field resonance corresponds to the edge mode. The inset shows the experimental arrangement with slowly swept field H_0 perpendicular to the stripes. Bottom: FMR map showing field dependence of resonance frequencies. For fields above $H_{\text{sat}}=0.15$ T, the lower frequency resonance is the edge mode.

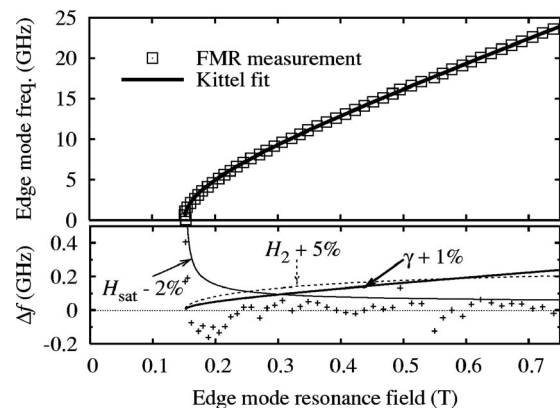


FIG. 3. Fit of the edge mode frequency to a Kittel-type model, using two parameters, H_{sat} and H_2 . The bottom panel shows the residual error of the fit and variations in the edge mode frequency for small changes in the parameters.

or more bulk modes in the center of the stripe. A precise determination of H_{sat} properties is obtained from the applied field dependence of the edge mode resonance frequency. As is the case with edge mode frequencies obtained by micromagnetic modeling,¹⁸ the measured field dependence of the edge mode resonance can be fitted quite accurately to a Kittel²⁰ form,

$$f = \gamma \mu_0 [(H_0 - H_{\text{sat}})(H_0 + H_2)]^{1/2}, \quad (1)$$

where H_2 is an effective stiffness field for out-of-plane motion of the magnetization near the edge and γ is the gyro-magnetic ratio. An example fit is shown in Fig. 3. In the fitting, we found that small variations in γ change the frequency given by Eq. (1) in ways that are very similar to a more substantial changes in H_2 (see the lower panel of Fig. 3). The values of H_{sat} and H_2 reported below were obtained by holding γ fixed at 29.3 GHz/T, which corresponds to a g value of 2.09. Although we cannot completely rule out the possibility that γ is affected by the patterning process near the edge, large variations in γ are deemed unlikely because the range of measured values of γ varies by less than 5% across the magnetic transition metal elements.

In Fig. 4, we plot measured values of H_{sat} ; these values vary by almost a factor of 2 as the etch depth and the side-

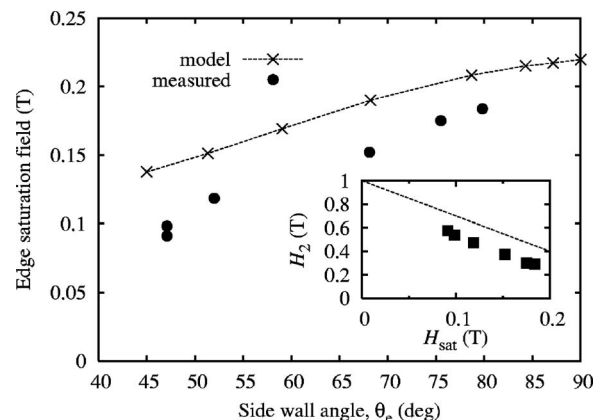


FIG. 4. Edge saturation field vs sidewall angle. The model values reproduce the trend observed in the measured values. The difference may be due to edge defects other than edge surface tilting. Inset: measured values of H_{sat} and H_2 have a linear relationship. The line represents the prediction of the macrospin model [Eq. (2)].

wall angle increase. For comparison, we also show results of micromagnetic calculations of H_{sat} for a range of sidewall angles in single stripes.²¹ For these calculations, we assumed $\mu_0 M_s = 1$ T and exchange stiffness $A = 13$ pJ/m. The model values plotted in Fig. 4 have been reduced by 5.9 mT, which corresponds to the field produced by the rest of the array of saturated stripes.

For the least etched sample, two edge modes with equal amplitudes were observed. From Fig. 1, it is clear that the sidewall angle is most sensitive to the etching conditions when the film is barely etched through. At this etch depth, θ_e and the edge properties will be most sensitive to any asymmetry in the etch process. Double edge modes were also observed in the spectra of a sample that was placed off center on the rotating platform during etching. Similar splitting of the edge modes were observed in some of the earliest spatially resolved studies of edge modes.¹⁴

In the inset of Fig. 4 we show empirically that the fit values of H_{sat} and H_2 are linearly related. This relationship is approximately consistent with the edge mode macrospin model,¹⁸ which predicts

$$H_2 = M_s - 3H_{\text{sat}}. \quad (2)$$

In the macrospin model, the edge mode magnetization is assumed to behave as if effective demagnetization factors govern the behavior of the edge magnetization. The relationship between H_{sat} and H_2 exists because these demagnetization factors sum to 1. This relationship given in Eq. (2) was previously found to be obeyed in model results where the edge geometry was varied by changing the thickness.¹⁸ Here, we have confirmed this relationship experimentally, changing the geometry through the patterning conditions.

In this letter, we have shown that the patterned edges of magnetic films have measurable magnetic properties, H_{sat} and H_2 , and shown quantitatively that these properties depend on the etching conditions used to create the edges. These results have important implications for generating

nanostructure arrays with uniform properties and for understanding the behavior of magnetic nanodevices.

- ¹R. C. Sousa and P. P. Freitas, IEEE Transl. J. Magn. Jpn. **37**, 1973 (2001).
- ²M. Yoshikawa, S. Kitagawa, S. Takahashi, T. Kai, M. Amano, N. Shimomura, T. Kishi, S. Ikegawa, Y. Asao, H. Yoda, K. Nagahara, H. Numata, N. Ishiwata, H. Hada, and S. Tahara, J. Appl. Phys. **99**, 08R702 (2006).
- ³M. Herrmann, S. McVitie, and J. H. Chapman, J. Appl. Phys. **87**, 2994 (2000).
- ⁴K. J. Kirk, M. R. Scheinfein, J. N. Chapman, S. McVitie, M. F. Gillies, B. R. Ward, and J. G. Tennant, J. Phys. D **34**, 160 (2001).
- ⁵J. O. Rantschler, P. J. Chen, A. S. Arrott, R. D. McMichael, W. F. Egelhoff, Jr., and B. B. Maranville, J. Appl. Phys. **97**, 10J113 (2005).
- ⁶J. W. Lau, M. Beleggia, M. A. Schofield, G. F. Neumark, and Y. Zhu, J. Appl. Phys. **97**, 10E702 (2005).
- ⁷J. Gadbois and J.-G. Zhu, IEEE Transl. J. Magn. Jpn. **31**, 3802 (1995).
- ⁸J. G. Deak and R. H. Koch, J. Magn. Magn. Mater. **213**, 25 (2000).
- ⁹M. T. Bryan, D. Atkinson, and R. P. Cowburn, Appl. Phys. Lett. **85**, 3510 (2004).
- ¹⁰R. P. Cowburn, J. Phys. D **33**, R1 (2000).
- ¹¹B. B. Maranville, R. D. McMichael, C. L. Dennis, C. A. Ross, and J. Y. Cheng, IEEE Transl. J. Magn. Jpn. **42**, 2951 (2006).
- ¹²B. B. Maranville, R. D. McMichael, S. A. Kim, W. L. Johnson, C. A. Ross, and J. Y. Cheng, J. Appl. Phys. **99**, 08C703 (2006).
- ¹³J. Jorzick, S. O. Demokritov, B. Hillebrands, M. Bailleul, C. Fermon, K. Y. Guslienko, A. N. Slavin, D. V. Berkov, and N. L. Gorn, Phys. Rev. Lett. **88**, 047204 (2002).
- ¹⁴J. P. Park, P. Eames, D. M. Engebretson, J. Berezovsky, and P. A. Crowell, Phys. Rev. Lett. **89**, 277201 (2002).
- ¹⁵M. Bailleul, D. Olligs, and C. Fermon, Phys. Rev. Lett. **91**, 137204 (2003).
- ¹⁶C. Bayer, J. P. Park, H. Wang, M. Yan, C. E. Campbell, and P. A. Crowell, Phys. Rev. B **69**, 134401 (2004).
- ¹⁷C. Bayer, S. O. Demokritov, B. Hillebrands, and A. N. Slavin, Appl. Phys. Lett. **82**, 607 (2003).
- ¹⁸R. D. McMichael and B. B. Maranville, Phys. Rev. B **74**, 024424 (2006).
- ¹⁹Y. Roussigné, S.-M. Chérif, and P. Moch, J. Magn. Magn. Mater. **268**, 89 (2004).
- ²⁰C. Kittel, Phys. Rev. **73**, 155 (1948).
- ²¹M. J. Donahue and D. G. Porter, OOMMF User's Guide, Version 1.0, Interagency Report NISTIR 6376, NIST, Gaithersburg, MD (Sept., 1999), <http://math.nist.gov/oommf>.